INFECTION AND IMMUNITY, Aug. 2011, p. 3273–3283 Vol. 79, No. 8
0019-9567/11/$12.00 doi:10.1128/IAI.05153-11

Analysis of the HD-GYP Domain Cyclic Dimeric GMP Phosphodiesterase Reveals a Role in Motility and the Enzootic Life Cycle of *Borrelia burgdorferi*▽†

Syed Z. Sultan,[1] Joshua E. Pitzer,[1] Tristan Boquoi,[1] Gerry Hobbs,[2] Michael R. Miller,[3] and M. A. Motaleb[1]*

Department of Microbiology and Immunology, Brody School of Medicine, East Carolina University, Greenville, North Carolina 27834[1]; Department of Statistics, West Virginia University, Morgantown, West Virginia 26506[2]; and Department of Biochemistry, Health Sciences Center, West Virginia University, Morgantown, West Virginia 26506[3]

Received 31 March 2011/Returned for modification 5 May 2011/Accepted 1 June 2011

HD-GYP domain cyclic dimeric GMP (c-di-GMP) phosphodiesterases are implicated in motility and virulence in bacteria. *Borrelia burgdorferi* possesses a single set of c-di-GMP-metabolizing enzymes, including a putative HD-GYP domain protein, BB0374. Recently, we characterized the EAL domain phosphodiesterase PdeA. A mutation in *pdeA* resulted in cells that were defective in motility and virulence. Here we demonstrate that BB0374/PdeB specifically hydrolyzed c-di-GMP with a K_m of 2.9 nM, confirming that it is a functional phosphodiesterase. Furthermore, by measuring phosphodiesterase enzyme activity in extracts from cells containing the *pdeA pdeB* double mutant, we demonstrate that no additional phosphodiesterases are present in *B. burgdorferi*. *pdeB* single mutant cells exhibit significantly increased flexing, indicating a role for c-di-GMP in motility. Constructing and analyzing a *pilZ pdeB* double mutant suggests that PilZ likely interacts with chemotaxis signaling. While virulence in needle-inoculated C3H/HeN mice did not appear to be altered significantly in *pdeB* mutant cells, these cells exhibited a reduced ability to survive in *Ixodes scapularis* ticks. Consequently, those ticks were unable to transmit the infection to naïve mice. All of these phenotypes were restored when the mutant was complemented. Identification of this role of *pdeB* increases our understanding of the c-di-GMP signaling network in motility regulation and the life cycle of *B. burgdorferi*.

The bacterial second messenger cyclic dimeric GMP (c-di-GMP) [bis(3′,5′)-cyclic diguanylic acid] has been associated with a wide range of adaptive processes, most notably, the regulation of virulence-related gene products and motility (17, 36, 76, 83, 92, 96). C-di-GMP exerts its regulatory function at the level of transcription, translation, protein activity, secretion, and/or protein stability via its interaction with various types of downstream effector molecules (36, 37, 80, 90). For example, in response to c-di-GMP, the *Escherichia coli* PilZ domain protein YcgR induces a counterclockwise (CCW) rotational bias by interacting with flagellar motor switch protein FliG, FliM, or MotA; however, in *Caulobacter crescentus*, a PilZ domain receptor, DgrA, was reported to destabilize the flagellar protein FliL, negatively affecting motility in response to c-di-GMP (7, 14, 22, 66, 80).

The levels of c-di-GMP are controlled by the opposing activities of diguanylate cyclase (DGC) and phosphodiesterase (PDE) enzymes. DGC enzymes synthesize c-di-GMP from two molecules of GTP, while PDEs hydrolyze c-di-GMP to pGpG or GMP. Open reading frames encoding DGC activity are characterized by the presence of a GGDEF protein domain. Proteins with PDE activity typically harbor either EAL or HD-GYP domains (36, 76, 83, 92). Although there are numerous reports on the characterization of GGDEF and EAL domain-containing proteins in diverse species of bacteria, only a few HD-GYP domain (HD-GYP; Pfam PF01966) proteins have so far been characterized, despite the fact that the HD-GYP domain proteins are also abundant in bacteria (28, 31). Comparative genome analyses indicated that a number of bacterial genomes encode proteins with the GGDEF domain but no identifiable EAL domain PDE (30, 31). A role for HD-GYP domain proteins in c-di-GMP hydrolysis was then proposed based on the distribution and numbers of GGDEF, EAL, and HD-GYP domains encoded by different bacteria and on the known activities of other members of the HD superfamily of enzymes as metal-dependent hydrolases (30). Experimental evidence of a role for the HD-GYP domain in c-di-GMP hydrolysis was provided through studies of *Xanthomonas* sp. RpfG (1, 77, 79). Two additional HD-GYP domain proteins, PA4108 and PA4718, from *Pseudomonas aeruginosa* also have been reported to be c-di-GMP PDEs (78). In each case, inactivation of these putative HD-GYP PDEs resulted in reduced motility and decreased virulence (1, 78, 79).

Synthesis of c-di-GMP in *Borrelia burgdorferi*, the Lyme disease spirochete, is controlled by the Hk1/Rrp1 two-component signal transduction system (31, 75), with Hk1 serving as the sensor histidine kinase component responsible for phosphorylating Rrp1, a diguanylate cyclase. Recent independent studies by Caimano et al. (10a), He et al. (35a), and Kostick et al. (45) indicate that these two gene products act cooperatively to promote spirochete survival in feeding ticks following acquisition. Interestingly, neither gene was required to establish in-

* Corresponding author. Mailing address: Department of Microbiology and Immunology, Brody School of Medicine, East Carolina University, Greenville, NC 27834. Phone: (252) 744-3129. Fax: (252) 744-3535. E-mail: motalebm@ecu.edu.

† Supplemental material for this article may be found at http://iai.asm.org/.

▽ Published ahead of print on 13 June 2011.

fection in mice by needle inoculation. Moreover, spirochetes lacking Hk1 were able to migrate out of the bite site into feeding nymphs but were killed within 36 h following ingestion. These results indicate that the function of Hk1/Rrp1 and c-di-GMP is likely to be restricted in the arthropod phase of the enzootic cycle. The presence of two distinct PDEs, PdeA (BB0363) and PdeB (BB0374), implies that the ability to modulate the intracellular levels of c-di-GMP is an important component of the spirochete's pathogenic strategy. Indeed, inactivation of the EAL domain containing c-di-GMP-specific PDE (*pdeA*) resulted in cells that were avirulent in mice, presumably as a result of their altered swimming pattern (91).

The motility of *B. burgdorferi* results from coordinated rotation of the periplasmic flagella residing between the outer membrane and the cell cylinder (12, 13, 18, 34, 46, 50). The motile behavior of *B. burgdorferi* and other spirochetes is unique and complex (12, 13). *In vitro*, *B. burgdorferi* exhibits three different swimming modes, i.e., running, flexing, and reversing (5, 12, 50, 58), with running occurring when the periplasmic flagellar motors at either end of the spirochete cell body rotate in opposite directions. Thus, the periplasmic flagella of the anterior ribbon rotates CCW and those of the posterior end rotate clockwise (CW) (as a frame of reference, a periplasmic flagellum is viewed from its distal tip along the filament toward insertion into the motor) (12, 13, 18, 50). The flex is a nontranslational mode that is often associated with bending of the cell body (33, 34, 58). During a flex, the motors at both ends rotate in the same direction; i.e., both rotate either CW or CCW (12, 23, 34, 50, 58). The spirochete flex is thought to be equivalent to the tumbling behavior displayed by *Escherichia coli* and *Salmonella enterica* serovar Typhimurium (8, 12, 23, 34, 50, 58). A reversal occurs in translating cells when the motors at either end simultaneously reverse their direction of rotation (12, 50). Phosphorylated CheY (CheY-P) plays a major role in regulating the direction in which flagellar motors rotate. Thus, a *B. burgdorferi cheY3* mutant (no CheY3-P) constantly runs whereas a CheY-P phosphatase *cheX* mutant (elevated CheY3-P) constantly flexes (58, 61, 67).

Bacterial motility is important for the colonization/disease process for numerous species of pathogenic bacteria, including *B. burgdorferi* (9, 10, 42, 52, 55, 62). *In vitro*, *B. burgdorferi* is able to traverse viscous gel-like media in which most other flagellated bacteria slow down or stop (44). *B. burgdorferi* is able to disseminate out of the site of inoculation and colonize diverse host tissues, such as joints, the nervous system, and the heart (33, 44, 86), due in part to its unique motility (12, 18, 34, 50–52, 91). However, motility is likely not required for spirochetes to survive or replicate in ticks (our unpublished observation; 19).

To better understand the importance of c-di-GMP signaling in the life cycle of *B. burgdorferi*, we characterized the single HD-GYP domain protein PdeB. We demonstrate that PdeB is a functional c-di-GMP PDE that binds c-di-GMP with high affinity and hydrolyzes it. By inactivating both *pdeA* and *pdeB* and using cell extracts in PDE assays, we established that *B. burgdorferi* encodes no additional PDE. Dark-field analysis of spirochetes lacking PdeB demonstrated that these cells exhibit significantly increased flexing, indicating a role for this PDE in modulating motility. Furthermore, although loss of PdeB did not significantly affect virulence in needle-inoculated mice, the mutant displayed a reduced ability to survive in *Ixodes scapularis* ticks. Ticks infected with the *pdeB* mutant were unable to transmit the infection into naïve mice, resulting in a failure to complete the mouse-tick-mouse infection cycle. Normal motility and survival in ticks were restored by complementation. Together, these data suggest a role for PdeB in tick-mediated transmission and imply that decreased levels of c-di-GMP may be important for the spirochete's survival postfeeding/postrepletion. Inactivation of the c-di-GMP receptor PilZ protein PlzA in the *pdeB* mutant background suggests a role for c-di-GMP/PlzA in chemotaxis signaling. Possible mechanisms by which PdeB, PlzA, and c-di-GMP alter motility and infectivity are discussed.

MATERIALS AND METHODS

Bacterial strains and growth conditions. Low-passage, virulent *B. burgdorferi* strain B31-A3-K2Δ*bbe002* (a kind gift from R. Rego and P. Rosa, Rocky Mountain Laboratories [RML], NIH) (72) was used as the wild type throughout this study. This strain is a derivative of A3-68 lacking circular plasmid 9 and linear plasmid 56 (lp56), with the *bbe002* gene inactivated using a P_{flgB}-*kan* cassette to increase the transformation frequency (43, 72). B31-A3-K2Δ*bbe002* is a derivative of strain B31 (21). The genome of the virulent B31 strain has been sequenced and was found to contain a total of 21 plasmids with 12 linear and 9 circular plasmids, in addition to the 960-kb linear chromosome (11, 25). *B. burgdorferi* was cultured in liquid Barbour-Stoenner-Kelly (BSK-II) medium; plating BSK-II was prepared using 0.6% agarose (57).

Construction of a *pdeB* mutant. Targeted inactivation of *pdeB* (1,140 bp; gene locus *bb0374*) was achieved by homologous recombination using a streptomycin resistance gene (*aadA*) as a marker (24). The *pdeB* gene was inactivated by replacing the first 1,040 bp of *pdeB* with the 792-bp *aadA* coding sequence using overlapping PCRs, as we recently described in detail (59). PCR was used to amplify 3 regions of DNA in 3 steps (not shown; see reference 59). In the first step, each DNA region was amplified separately using PCR pairs P1-P2 (5′-flanking DNA, *bb0373*), P3-P4 (*aadA* coding sequence from plasmid pKFSS1), and P5-P6 (3′-flanking DNA, *pfs*). Primers P2, P3, P4, and P5 contain several overlapping base pairs (see below). During step 2, a PCR product was obtained using primers P1-P4 and the purified DNA products for *bb0373* and *aadA* as templates. In step 3, the final PCR product was obtained using primers P1-P6 and purified DNA products *bb0373-aadA* and *pfs* as templates. The primer sequences (5′-3′) are as follows: P1, AGACTTTGCAAAAAAATAAT; P2, CGCTTCCCTCATTTATTCCCTTGAAATTAAGCTC; P3, TCAAGGGAATAAATGAGGGAAGCGGTGATCGCCG; P4, TGGTATAGATTGTTATTTGCCGACTACCTTGGTG; P5, GTCGGCAAATAACAATCTATACCAAATACAAATAC; P6, AATCAATATTTGTATAGCCTATATC1. The final PCR yielded a 2,891-bp product that was gel purified and cloned into the pGEM-T Easy vector (Promega Inc.). The deletion-insertion was in frame. The integrity of the *pdeB* inactivation plasmid was confirmed by PCR and restriction mapping. NotI-digested DNA was electroporated into wild-type competent cells and plated on plating BSK containing 200 μg ml^{-1} kanamycin plus 100 μg ml^{-1} streptomycin as described previously (57). Resistant clones were analyzed by PCR for the confirmation of homologous recombination. PCR-positive mutants were further examined for their plasmid contents using 21 sets of primers to detect 21 linear and circular plasmids (100).

Complementation of *pdeB* mutant. To complement the *pdeB* mutant, the promoter of the *pdeB* operon (P_{pdeB}; 345 bp upstream from the ATG start codon of the *pdeB* gene) (74) and the coding sequence of *pdeB* were amplified by PCR with primers *Bb0373-BamHI-F* (**GGATCC**GTGAATGCATCTTCCATCCCA) and *Bb0374-Pst-R* (**CTGCAG**TTATATAATATCTATTAAAGAA). BamHI and PstI sites are in bold font. The 1,499-bp PCR product (P_{pdeB}-*pdeB*) was ligated into pGEM-T Easy. The P_{pdeB}-*pdeB* DNA was then inserted into shuttle vector pBSV2G (41, 91) using PstI and BamHI restriction digestion, yielding pBSbb0374. Fifty micrograms of the resultant plasmid was electroporated into the *pdeB*::*aadA* competent cells. Transformants were selected on solid growth medium containing 200 μg ml^{-1} kanamycin, 100 μg ml^{-1} streptomycin, and 40 μg ml^{-1} gentamicin. Resistant transformants were analyzed by PCR for the presence of Str^r, Gm^r, and *pdeB*. To confirm that the plasmid was complementing in *trans*, the pBSVbb0374 shuttle vector was rescued from complemented *pdeB*$^+$ cells, transformed, and then purified from *E. coli* and the integrity of P_{pdeB}-*pdeB*

was verified by restriction digestion. Positive transformants were further examined for their plasmid content by PCR.

Dark-field microscopy and swarm plate assays. Exponentially growing *B. burgdorferi* cells were observed under a dark-field microscope (Zeiss Axio Imager M1) connected to an AxioCam digital camera and video recorded. The flex rate was determined by determining the mean number of flexes per minute ± the standard deviation. At least 12 cells of each strain were analyzed. A paired Student *t* test was used to determine statistical significance (a *P* value for the difference between the wild type and the mutant). Swarm plate assays were performed as described previously (50, 52, 57, 58). Approximately 1×10^6 cells in a 5-μl volume were spotted onto a 0.35% agarose plate containing plating BSK-II medium diluted 1:10 in phosphate-buffered saline (PBS) without divalent cations. Because *B. burgdorferi* is a slow-growing organism with an 8- to 12-h generation time, swarm plates were incubated for 6 days at 35°C in a 2.5% CO_2 humidified incubator (57, 91).

Reverse transcription (RT)-PCR. Exponentially growing cultures of *B. burgdorferi* were treated with RNAprotect, and then total RNA was isolated using the RNeasy minikit (Qiagen Inc.). Contaminating DNA in the RNA samples was removed by RNase-free Turbo DNase I (Ambion, Inc.) digestion for 3 h at 37°C, followed by RNeasy mini purification. For RT-PCR, cDNA was prepared from 1 μg of RNA using the Bio-Rad cDNA synthesis kit according to the manufacturer's protocol. The iCycler detection system (Bio-Rad Inc.) was used to measure the transcript level of the test genes in wild-type, *pdeB* mutant, and complemented cells according to the manufacturer's instructions. The *B. burgdorferi* gene for enolase was used as a reference (60). The gene-specific primers (5′-3′) were (i) BB0374 qRT F (TTATTCATTCGGTAAATACAGCTATC) and BB0374 qRT R (CTAGTTCTTCCTCAGTTAATGCTTCT) and (ii) RT-enolase-F (TGGAGCGTACAAAGCCAACATT) and RT-enolase-R (TGAAAAA CCTCTGCTGCCATTC). The relative level of expression was calculated using the $2^{-\Delta\Delta CT}$ method (54, 84).

Sodium dodecyl sulfate-polyacrylamide gel electrophoresis (SDS-PAGE) and Western blot analysis. SDS-PAGE and Western blotting with an enhanced chemiluminescent detection method (GE Healthcare) were carried out according to the manufacturer's instructions. The concentration of proteins in the cell lysates was determined by a Bio-Rad protein assay kit. Unless noted otherwise, 10 μg of lysates was loaded in each lane for SDS-PAGE, transferred to polyvinylidene fluoride membranes, and subjected to Western blotting using specific antibodies. The following antibodies were kindly provided by other investigators: polyclonal anti-Pfs by B. Stevenson (University of Kentucky, Lexington, KY), monoclonal anti-FlaB (H9724) by A.G. Barbour (University of California, Irvine, CA), monoclonal anti-DnaK by J. Benach (SUNY, Stony Brook, NY), polyclonal anti-MotB by J. Carroll (NIH at RML, Hamilton, MT), polyclonal FliG1 and FliG2 by C. Li (SUNY, Buffalo, NY), and polyclonal FliM by D. Blair (University of Utah, Salt Lake City, UT). The specific reactivity of these antibodies to *B. burgdorferi* CheX, CheY3, Pfs, FlaB, MotB, FliG1, FliG2, and FliM has been reported previously (16, 50, 52, 56, 58, 60, 74, 82).

R-PdeB protein expression and PDE assays. For overexpression and purification of recombinant PdeB (R-PdeB) protein, the coding sequence of *pdeB* was amplified without the first ATG start codon by PCR using primers R-374-Bam-F (**GGATCC**CAAAATTCTGAAAGCATTAT) and R-374-Pst R (**CTGCAG**TTA TATAATATCTATTAAAGAATA), creating a BamHI and a PstI site (bold), respectively. For overexpression and purification of the HD-GYP domain (amino acids [aa] 90 to 305) of PdeB, the *pdeB* coding sequence was amplified without the first 89 and the last 75 aa residues by PCR using primers R-374-HDGYP-Bam-F (**GGATCC**TATGAAAATTGCAAAAGAAATAAA) and R-374-HDGYP-Pst-R (**CTGCAG**TAAAGTCTAAGGGACAAGAAGATAT), creating a BamHI and a PstI site (bold), respectively. The amplified DNA fragments were ligated into *E. coli* expression vector pMAL-c2X (New England BioLabs) using BamHI and PstI. The recombinant expression vectors constructed for PdeB and the HD-GYP domain were named p*bb0374*-MAL and p*bbHDGYP*-MAL, respectively. The recombinant expression vectors were analyzed by restriction digestion to confirm their integrity. *E. coli* cells containing p*bb0374*-MAL or p*bbHDGYP*-MAL were induced with 0.25 mM isopropyl-β-D-thiogalactopyranoside at 30°C for 4 h and purified on amylose resin (New England BioLabs). Purified proteins were concentrated and dialyzed in PDE buffer (75 mM Tris-HCl [pH 8], 10 mM $MgCl_2$, 25 mM KCl, 250 mM NaCl). Purified R-PdeB or HD-GYP protein was resolved by SDS-PAGE to determine protein concentration and purity.

PDE assays of wild-type, *pdeB* mutant, complemented *pdeB*$^+$, and *pdeA pdeB* double mutant cell extracts were performed as described previously (15, 91), with minor modifications. Briefly, cell pellets were washed once with PBS and resuspended in PDE assay buffer (250 mM NaCl, 25 mM Tris-HCl [pH 8], 10 mM $MgCl_2$, 25 mM KCl, 10% glycerol). Cells were lysed by a combination of French press and sonication. Lysed cells were centrifuged at 100,000 × *g* for 1 h, and the protein concentration in the supernatants was determined using a Bio-Rad protein assay kit. Synthesis of radiolabeled c-di-GMP substrate for PDE assays was performed as described previously (49, 91) and approved by the East Carolina University Radiation Safety Subcommittee. An *E. coli* clone carrying *P. aeruginosa* His_6-WspR, which has high diguanylate cyclase activity, was affinity purified as described previously (47, 49, 91). ^{33}P-labeled c-di-GMP was prepared by incubating 20 μg of His_6-WspR, 100 mCi of [α-^{33}P]GTP (3,000 Ci mmol^{-1}; 10 mCi ml^{-1}; Perkin-Elmer) in 50 mM Tris-HCl (pH 7.5)–250 mM NaCl–10 mM $MgCl_2$–1 mM dithiothreitol for 4 h at 25°C. The reaction mixture was then incubated with 20 units of calf intestine alkaline phosphatase (New England BioLabs) for 1 h at 25°C to hydrolyze unreacted GTP. The reaction was stopped with 0.5 M EDTA, and the product was passed through an Ultrafree MC-5000 column (Millipore Inc.). PDE assays were performed as described previously (91, 94). R-PdeB protein (2 μg) or *B. burgdorferi* crude extract (4 μg) was incubated with ^{33}P-labeled c-di-GMP with or without 50 mM $MnCl_2$ for different periods of time. A no-enzyme or unrelated-protein (maltose binding protein [MBP]-FlhF) negative control and a *Vibrio cholerae* PDE His_6-CdpA (1.5 μg) positive control were used (91, 93). Reaction products (1 μl) were spotted and separated by thin-layer chromatography (TLC) using polyethyleneimine-cellulose plates in 1.5 M KH_2PO_4 (pH 3.65) buffer. The plates were air dried, and then phosphorimaging and volume analysis using Image Quant TL v2003 were done. To determine the K_m, R-PdeB was incubated with 2 to 70 nM ^{33}P-labeled c-di-GMP for up to 30 min, reactions were stopped every 5 min, the products were subjected to TLC, and the results were analyzed using GraphPad Prism 5 (Michaelis-Menten equation) as described previously (15, 91, 94). To determine the substrate specificity of R-PdeB, 15 to 30 nM ^{3}H-labeled cGMP (Perkin-Elmer) was incubated with 6 mg of R-PdeB for 30 min to overnight and the reaction product was separated by TLC as described previously (91, 94).

Experimental mouse-tick-mouse infection model of *B. burgdorferi*. Five-week-old female C3H/HeN mice were purchased from Charles River Laboratories, Durham, NC, and housed in the East Carolina University animal facility at the Brody School of Medicine according to the institutional guidelines for the care and use of laboratory animals. For infection via needle, 5×10^2 to 5×10^4 *in vitro*-grown spirochetes were injected subcutaneously as described previously (21, 40, 73). The number of spirochetes was determined using a Petroff-Hausser chamber, and each clone was verified for retention of lp25, lp28-1, and lp36 plasmids. Mice were bled 2 weeks postinfection, and sera against *B. burgdorferi* antigens were tested to determine infectivity as described previously (21, 85). Reisolation of spirochetes from mouse ears, joints, and bladders was performed at 4 weeks postinfection as previously described (91) to assess the ability of spirochetes to infect mice. Mouse tissues were incubated in BSK-II growth medium for up to 35 days, and the presence of spirochetes was determined by dark-field microscopy. Reisolated clones were genotyped using PCR as described above.

For tick infection studies, naïve *I. scapularis* larvae were purchased from Oklahoma State University. Two independent experiments were performed with ticks. Ticks were kept at 23 to 24°C under a 14/10 light/dark photoperiod in a humidified chamber with 85 to 90% relative humidity. Approximately 150 larval ticks were fed to repletion on spirochete-infected mice for 5 to 7 days, allowed to fall off, and collected. One subset of larvae was dissected 7 days after repletion, and the isolated midguts were analyzed by indirect immunofluorescence assays (IFA) for the presence of spirochetes (87, 91). A second subset of fed larvae were surface sterilized using 3% H_2O_2, followed by 70% ethanol; crushed in BSK-II medium; and plated to determine the number of CFU per tick. The remaining fed larvae were allowed to molt to nymphs. Those nymphs were then fed to repletion on naïve mice (five-week-old female C3H/HeN mice), allowed to fall off, and collected. Subsets of nymphs were dissected 7 to 9 days after repletion, and the isolated midguts were analyzed by IFA for the presence of spirochetes. Fed nymphs were surface sterilized as described above, crushed in BSK-II medium, and plated to determine the number of CFU per tick. Mice were bled 2 weeks after nymph infection for immunoblot analysis of mouse sera, and reisolation of *B. burgdorferi* from mouse ear, bladder, and joint tissues was performed 4 weeks postinfection.

Determination of 50% infective dose (ID_{50}) and statistical analysis. The dose required to infect 50% of the mice inoculated was experimentally determined for the wild-type and *pdeB* mutant strains as described previously (40, 68, 71). The data from the ID_{50} infection experiment and the single-dose infection experiment for each strain were combined for estimation of the ID_{50}. Comparison of strain ID_{50} values was done using a generalized linear model with a probit link function. This method is also known as probit regression (40), and in it we assume identical slopes in the response/log-dose relationship but different intercepts for each strain. Graphically, those assumptions manifest themselves as

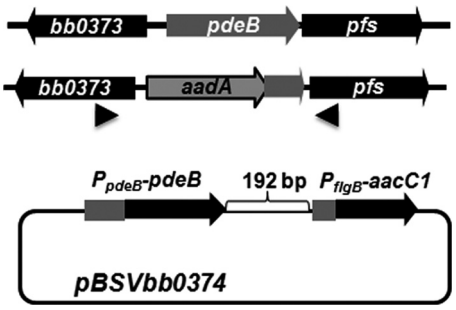

FIG. 1. Construction and complementation of *pdeB*. Schematic representation of *pdeB* and its neighboring genes in wild-type *B. burgdorferi* is shown at the top. The first 1,040 bp of the *pdeB* gene is deleted to insert a 792-bp streptomycin resistance gene (*aadA*) in frame (middle panel). The approximate locations of one of the primer sets that were used to confirm *pdeB* inactivation (see Fig. 2) are shown by the arrowheads. Complementation plasmid pBSVbb0374 containing the *pdeB* promoter (P_{pdeB}) that drives the expression of the *pdeB* gene was used to complement the *pdeB* mutant (bottom panel).

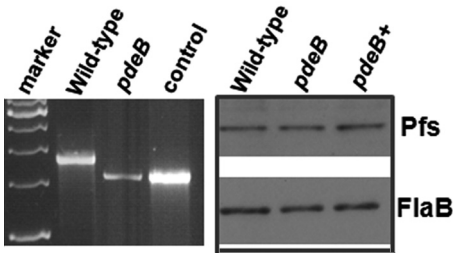

FIG. 2. Confirmation of *pdeB* inactivation and assessment of polar effect. (Left panel) PCR was used to confirm the deletion of the *pdeB* gene and integration of *aadA* (Str^r). The locations of the PCR primers used are shown in Fig. 1. A 792-bp DNA fragment containing the *aadA* coding sequence was inserted after the deletion of a 1,040-bp fragment from the *pdeB* gene. Marker lane, 1-kb DNA ladder (Fermentas Life Sciences). Wild-type lane, wild-type DNA (2,333 bp); *pdeB* lane, *pdeB*::*aadA* DNA (1,541 bp); control lane, *pdeB*::*aadA* DNA (1,541 bp) that was electroporated into wild-type cells (positive control). (Right panel) Lack of a polar effect on BB0375 (Pfs; 27 kDa) protein expression in *pdeB* mutant cells was determined by Western blotting using anti-Pfs antiserum (74). FlaB (41 kDa) was used as a loading control for the strains indicated.

dose-response curves with lateral shifts corresponding to the changes in intercept. Additionally, an overdispersion parameter was fitted in order to accommodate greater homogeneity of infection rates than would otherwise be permitted by the model. All calculations were carried out using JMP V9 software (SAS Institute Inc., Cary, NC).

Artificial inoculation of ticks by immersion. Approximately 150 larval ticks were artificially infected by immersion (in duplicate) in equal-density exponential-phase *B. burgdorferi* cultures as described previously (6, 69, 91), except that larval ticks were equilibrated to a lower relative humidity overnight before immersion to enhance spirochete uptake. Ticks were fed to repletion on separate naïve mice for 5 to 7 days, allowed to fall off, and collected. One subset of larvae were crushed 7 days after repletion and analyzed by IFA for the presence of spirochetes (87, 91). A second subset of fed larvae were surface sterilized using 3% H_2O_2, followed by 70% ethanol; crushed in BSK-II medium; and plated to determine the number of CFU per tick. Serum was collected at 2 weeks after repletion, and mouse tissues were harvested at 4 weeks after repletion as described above. In determining the total number of spirochetes per fed tick, 5 ticks were analyzed for each strain and the results are expressed as the mean ± the standard deviation.

IFA. Ticks were dissected in10 μl PBS–5 mM $MgCl_2$ on Teflon-coated microscope slides, mixed by pipetting, and then air dried (91). To avoid quenching by hemin in the blood, dissected tick contents were 10-fold serially diluted (P. Policastro, RML, NIH, personal communication). Slides were blocked with 0.75% bovine serum albumin in PBS–5 mM $MgCl_2$ and washed with PBS–5 mM $MgCl_2$. Spirochetes were detected using a 1:100 dilution of goat anti-*B. burgdorferi* antiserum labeled with fluorescein isothiocyanate (Kirkegaard & Perry Laboratories). Images were captured using a Zeiss Axio Imager M1 microscope coupled with a digital camera (91).

RESULTS

Inactivation and complementation of *pdeB*. *B. burgdorferi* genome organization, as well as RT-PCR analyses, indicated that *pdeB* is cotranscribed with other genes in an operon, *pdeB-pfs-metK-luxS* (25, 38, 74). A σ^{70} promoter has also been located directly upstream of *pdeB* (74). In this operon, *pdeB* is predicted to be a PDE (see below), *pfs* encodes a nucleosidase which is essential for depleting toxic metabolic by-products, *metK* is essential for normal cell growth and septation, and the *luxS*-encoded enzyme synthesizes 4,5-dihydroxy-2,3-pentanedione/autoinducer 2 (4, 38, 65, 74). A *luxS* mutant was constructed and reported to be not essential for infecting *I. scapularis* ticks or mice or transmission between these hosts (38). The expression of genes in the *pdeB* operon has also been reported to be modulated as a function of the growth phase (74). However, whether the HD-GYP domain-containing protein PdeB is a functional PDE has not been reported. To determine if *pdeB* functions in the *B. burgdorferi* enzootic life cycle, we inactivated this gene using allelic-exchange mutagenesis (Fig. 1) (59) by replacing a 1,040-bp fragment of the gene with the streptomycin resistance *aadA* gene (24) without its promoter. We found that this strategy prevents polar effects on the expression of downstream genes (59). PCR analysis confirmed that the Str^r marker (*aadA* coding sequence) was correctly inserted within the *pdeB* gene, as expected (Fig. 2, left panel). To assess whether insertion of *aadA* exerted an unexpected polar effect on the expression of *pfs* (immediately downstream from *pdeB*), Western blot analysis was conducted using antiserum raised against Pfs (74). Western blotting results indicated that the synthesis of Pfs was not altered in the *pdeB* mutant (Fig. 2, right panel). These results indicated that the in-frame insertion of the *aadA*/Str^r marker did not induce a polar effect.

To demonstrate that the *pdeB* mutant phenotype (see below) was due solely to the mutation and not due to a secondary alteration elsewhere, we complemented the mutant in *trans* using a shuttle vector, pBSV2G (Fig. 1, bottom) (20, 88, 91). Real-time PCR analysis indicated that *pdeB* transcripts were detected in wild-type cells but not in mutant cells, confirming inactivation of *pdeB*; *pdeB* transcripts in complemented $pdeB^+$ cells were elevated approximately 5-fold above the level in wild-type cells, indicating overexpression from the multicopy vector (data not shown; see below) (95). To confirm retention of *B. burgdorferi* endogenous plasmids (63, 70) in the *pdeB* mutant and complemented strains, PCR-based plasmid profiling using each of the plasmid-specific primers was employed (70, 100). The plasmid profiles of the wild-type, *pdeB* mutant, and $pdeB^+$ strains were the same, confirming the retention of all of the plasmids required for infectivity (not shown; see below).

Analysis of *pdeB* mutant phenotype. To determine if a mutation in *pdeB* altered *B. burgdorferi* motility, the mutant cells were analyzed using dark-field microscopy and swarm plate

TABLE 1. *pdeB* mutant cells exhibit a significantly increased flex rate[a]

Strain	Swimming pattern	No. of flexes/min[b]	*P* value
Wild type	Run-pause/flex-reverse	5.0 ± 1.7	0.002
pdeB mutant	Run-pause/flex-reverse	9.7 ± 3.3	
Complemented *pdeB*$^+$	Run-pause/flex-reverse	5.5 ± 1.6	

[a] See cell videos in the supplemental material.
[b] The flex rate was determined as the mean number of flexes per minute ± the standard deviation. For convenience, flexing is defined as cells bending in the middle or exhibiting a twisted or circular morphology with no positive displacement.

motility assays (Table 1; see Fig. S1 in the supplemental material). As shown in Table 1, the mutant cells ran, flexed, and reversed as did the wild-type cells; however, their rate of flexing was significantly higher than that of the wild-type cells (5 versus 10 flexes/min; *P* value, 0.002). When a *B. burgdorferi* cell flexes, it becomes distorted or bent at the center (see videos S1 to S3 in the supplemental material for wild-type, *pdeB* mutant, and complemented *pdeB*$^+$ cells) (33, 34, 58). In the swarm plate assays, the mutant swarm diameters were not significantly ($P = 0.074$) different from those of wild-type cells (see Fig. S1). As expected, the motility of the complemented *pdeB*$^+$ cells was restored to the wild-type phenotype (Table 1; see Fig. S1 and videos S1 to S3). Together, these results indicate a role for *pdeB* in motility and that the mutant's phenotype was due solely to this mutation and not to a secondary alteration elsewhere.

Loss of PlzA and PdeB results in constant flexing motility. In other species of bacteria, PilZ proteins were reported to control motility in response to changes in the level of c-di-GMP (3, 7, 14, 22, 66). *B. burgdorferi* possesses a c-di-GMP binding PilZ protein, PlzA (26, 68). To determine if PlzA can function in response to c-di-GMP to regulate *B. burgdorferi* motility, we constructed a *plzA* mutant in the *pdeB* mutant background by introducing one inactivated plasmid (*plzA*::*Pl-kan*) into the other mutant cells (*pdeB*::*aadA*). The *plzA* single mutant exhibits a normal swimming pattern but reduced swarming motility (68). The *B. burgdorferi plzA pdeB* double mutant cells exhibited a constant-flexing motility phenotype similar to the phenotype of *cheX* mutant cells (see the constant-flexing *cheX* mutant and *plzA pdeB* double mutant cell videos) (58). To determine if the increased flexing motility exhibited by the *pdeB* single mutant or the *plzA pdeB* double mutant was due to diminished levels of a motility/chemotaxis protein, we performed Western blotting using specific antiserum. As shown in Fig. 3, the expression of prominent motility or chemotaxis protein FlaB, FliG2, FliG1, FliM, MotB, CheY3, or CheX was not altered in the *pdeB* or *plzA pdeB* mutant cells. These results suggest that the altered motility exhibited by those mutants is not due to the reduced expression of major motility/chemotaxis proteins. However, it is possible that the constant-flexing phenotype exhibited by the double mutant cells is due to inhibition of CheX activity.

PdeB is a functional c-di-GMP PDE, and PdeA and PdeB are the only active PDEs in *B. burgdorferi*. Recently, we reported that the EAL domain-containing protein PdeA is a functional c-di-GMP-specific PDE (91). HD-GYP domain proteins have been reported to possess c-di-GMP PDE activity in *Xanthomonas campestris* and *P. aeruginosa* (77, 78). To determine if PdeB is an active PDE, we performed PDE assays using purified R-PdeB, as well as *B. burgdorferi* mutant cell extracts, as we and others previously described (15, 91, 94). Purified (greater than 90% pure; see Fig. 4B, right panel) recombinant full-length PdeB (379 aa) or only the HD-GYP domain (aa 90 to 305) and crude cell extracts prepared from wild-type, *pdeB* mutant, and *pdeB*$^+$ complemented cells were tested for the ability to hydrolyze ^{33}P-labeled c-di-GMP. As shown in Fig. 4A, the wild-type crude extract hydrolyzed c-di-GMP to GMP, indicating PDE activity (29 ± 3 fmol/mg/min; wild-type lanes). Addition of 50 mM $MnCl_2$ to the reaction mixture enhanced the PDE activity, which is indicative of metal-dependent PDE activity (all lanes). *pdeB* mutant extracts also hydrolyzed c-di-GMP to GMP but at a lower rate (19 ± 1.9 fmol/mg/min) than the wild-type extracts (Fig. 4A, lanes *pdeB*), indicating the presence of another PDE in these mutants. *pdeB*$^+$ complemented cell extracts rapidly hydrolyzed ^{33}P-labeled c-di-GMP (67 ± 1.7 fmol/mg/min; lanes *pdeB*$^+$), indicating that the reduction of ^{33}P-labeled c-di-GMP hydrolysis in *pdeB* mutant cells was restored upon complementation. *pdeB*$^+$ cell extracts exhibited greater-than-wild-type PDE activity, likely because *pdeB* was overexpressed in the complemented cells. These results indicated that PdeB is a functional PDE. To further confirm that PdeB is a c-di-GMP PDE, purified full-length PdeB or only the HD-GYP protein was assayed for the ability to hydrolyze ^{33}P-labeled c-di-GMP (Fig. 4B and C). The full-length protein or only the functional do-

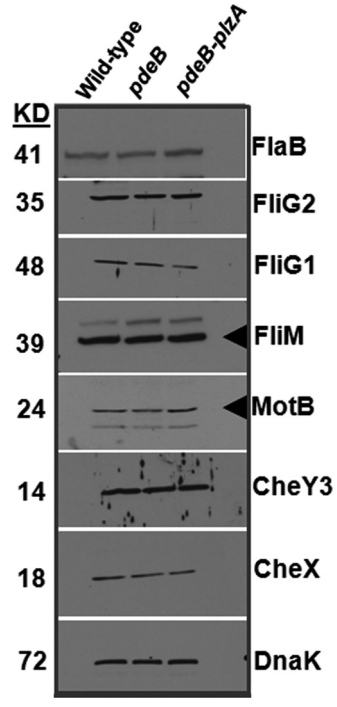

FIG. 3. The expression of prominent motility or chemotaxis proteins was not altered in *pdeB* or *plzA pdeB* mutant cells. Cell lysates from the indicated strains were probed with antibodies specific for the proteins shown on the right side of each Western blot. The molecular size (in kDa) of each protein is provided on the left side of each blot.

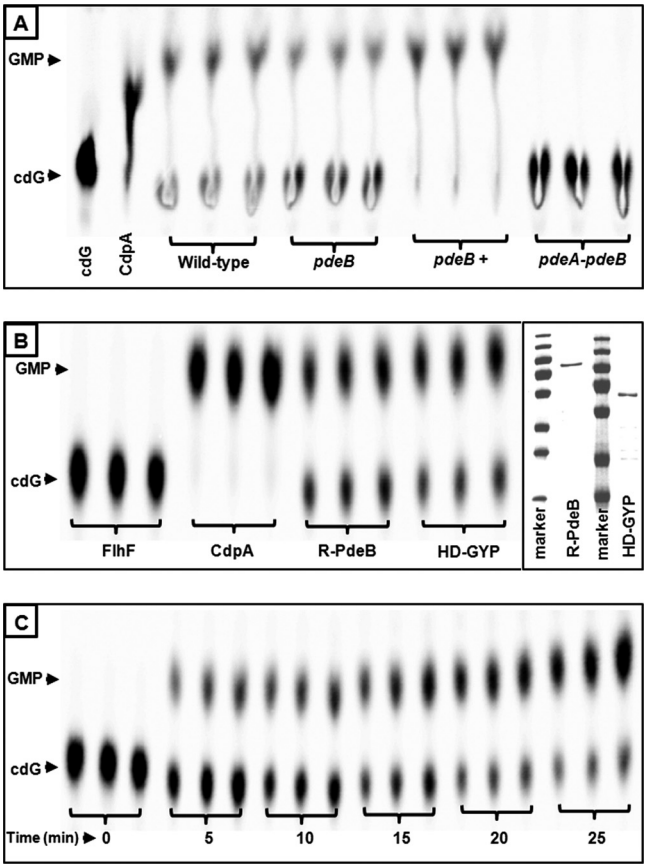

FIG. 4. *pdeB* exhibits PDE activity. (A) Representative TLC chromatogram of the PDE assay. cdG represents c-di-GMP. All lanes contain 50 mM $MnCl_2$. A *V. cholerae* PDE, CdpA, was used as a positive control. Wild type, *pdeB*, *pdeB*$^+$, and *pdeA pdeB* refer to extracts of the corresponding cells. Cell extracts were incubated with ^{33}P-labeled c-di-GMP for 20 min. (B) Representative TLC assay (20 min) of purified recombinant (lanes R-PdeB) or only the HD-GYP domain (lanes HD-GYP) protein. All lanes contained $MnCl_2$, except the positive control, CdpA. The R_f values for the nucleotides in these assays (c-di-GMP, 0.31; GMP, 0.55) agree well with published reports (91, 93, 94). MBP-FlhF was used as a negative control (lane FlhF). The right panel shows the purified R-PdeB (~87 kDa) and HD-GYP (~68 kDa) proteins. PageRuler plus protein markers were obtained from Fermentas Life Sciences. (C) Representative time course (0 to 25 min) TLC assay of the R-PdeB protein.

main hydrolyzed ^{33}P-labeled c-di-GMP to GMP (Fig. 4B and C). The addition of $MnCl_2$ enhanced the PDE activity, establishing that PdeB is a metal-dependent c-di-GMP PDE (all lanes).

Full-length R-PdeB was assayed with different concentrations of ^{33}P-labeled c-di-GMP, and the K_m value was calculated to be 2.9 nM, indicating a high affinity for c-di-GMP. The positive control, CdpA, rapidly hydrolyzed c-di-GMP, and negative controls without added protein or with an unrelated FlhF protein failed to hydrolyze c-di-GMP (Fig. 4A and B) (91, 93). Furthermore, ^{3}H-labeled cGMP was used to determine if PdeB is a c-di-GMP-specific PDE. ^{3}H-labeled cGMP was not hydrolyzed by R-PdeB, even when the reaction mixture was incubated for a prolonged period of time (overnight; data not shown), suggesting that PdeB is a c-di-GMP-specific PDE.

To determine if *B. burgdorferi* possesses only two PDEs (PdeA and PdeB), we constructed a *pdeA*::*Pl-kan-pdeB*::*aadA* double mutant by introducing one inactivated plasmid into the other mutant cells. The *pdeA pdeB* double mutant cell motility phenotype was indistinguishable from that of the *pdeB* single mutant. Extracts from *pdeA pdeB* double mutant cells failed to hydrolyze ^{33}P-labeled c-di-GMP, even when the reaction mixture was incubated for extended times (up to 4 h) (Fig. 4A, *pdeA pdeB* lanes; data not shown). Therefore, it is likely that PdeB and PdeA are the only two active c-di-GMP PDEs in *B. burgdorferi*.

***pdeB* mutant cells are not attenuated to establish an infection in mice.** In order to evaluate the infection potential of the *pdeB* mutant, groups of C3H/HeN mice were challenged by subcutaneous injection with 10-fold increasing doses of wild-type, *pdeB* mutant, or isogenic complemented *pdeB*$^+$ cells to determine the ID_{50}. At 2 weeks postinoculation, the mice were bled and their sera were assessed for reactivity with *B. burgdorferi* antigens. *B. burgdorferi* membrane protein A, also known as P39, was used as a marker of infection in animals (40, 85). To confirm the serological results, mice were sacrificed at 4 weeks postinoculation and tissue (ear, joint, and bladder) samples were aseptically isolated and assessed for the presence/absence of *B. burgdorferi* using dark-field microscopy. Serology results correlated well with reisolation of spirochetes from the tissues examined (Table 2 and not shown). *pdeB* mutant cells did not show a significant increase in the ID_{50} compared to parental wild-type cells ($P = 0.3976$; Table 2). These results indicate that the *pdeB* mutant is not significantly attenuated in virulence relative to the parental wild-type strain or the complemented *pdeB*$^+$ strain.

***pdeB* mutant cells are unable to complete the mouse-tick-mouse infection cycle.** The *B. burgdorferi* infectious life cycle includes persistent infection of and survival within tick and mammalian hosts. Because persistent infection of the mammalian host represents only one facet of the spirochete's enzootic life cycle, a more comprehensive evaluation of the behavior of *pdeB* mutant strains in the tick vector was warranted. To perform such an evaluation, naïve larval ticks were allowed to feed on mice that were infected with the wild-type, mutant, or complemented strain. Upon larval repletion, the majority of the ticks were allowed to advance naturally through the month-long molting process. At 7 days postfeeding, a subset of fed larvae was assessed for the survivability of spirochetes using IFA as well as squashing and plating of triturated ticks to count viable spirochetes (Table 3 and data not shown; see Fig. S2 in the supplemental material). While the numbers of spirochetes in ticks that fed on the wild-type and complemented *pdeB*$^+$ strains were similar, the number of viable spirochetes was

TABLE 2. *pdeB* mutant cells are not significantly attenuated in virulence in needle-inoculated C3H/HeN mice

Strain	No. of infected mice/total			ID_{50}
	5×10^{2a}	5×10^{3a}	5×10^{4a}	
Wild type	2/8	5/7	6/6	1.7×10^3
pdeB mutant	1/8	4/7	6/6	2.9×10^3
Complemented *pdeB*$^+$	Not done	4/7	6/6	Not done

[a] No. of spirochetes/mouse.

TABLE 3. *pdeB* mutant cells are unable to complete the mouse-tick-mouse infection cycle

Strain	No. of spirochetes/mouse	% of mice infected	% of ticks infected	Mean no. of spirochetes/nymph ± SD	No. of nymphs per mouse	No. of mice infected/total
Wild type	5×10^4	100	50	20,900 ± 11,172	30	4/4
pdeB mutant	5×10^5	100	50	4,466 ± 702	30	0/4
Complemented *pdeB*$^+$	5×10^4	100	60	15,666 ± 757	30	2/4

5-fold lower in ticks that fed on the mutant-infected mice (Table 3). The percentage of ticks infected with the wild-type, mutant, or complemented strain was approximately 50%; these results indicated that a mutation in *pdeB* resulted in cells that were deficient in survival in ticks (Table 3). The subset of fed larvae that molted to nymphs was examined for the spirochetes' ability to migrate from the ticks to naïve mice to complete the mouse-tick-mouse infection cycle (below).

Ticks infected with *pdeB* mutant cells are unable to transmit the infection to naïve mice. In the normal *B. burgdorferi* infectious cycle, mice are infected when spirochete-laden ticks bite them. We determined whether infected nymphs are able to transmit the spirochetes to naïve mice. Thirty nymphs of each group of wild-type, *pdeB* mutant, and complemented *pdeB*$^+$ strains were allowed to feed on a naïve mouse ($n = 4$) to determine spirochete transmission from ticks to the mammalian hosts (Table 3). Although the percentage of ticks infected with all 3 strains was approximately 50%, the mutant-infected ticks failed to transmit the infection to any mice, whereas wild-type-infected ticks were able to transmit the infection to all mice, as confirmed by reisolation of spirochetes from sacrificed mouse tissue (ear, joint, and bladder) specimens (Table 3). The *pdeB*$^+$ spirochete-infected ticks were also able to transmit the infection to 2/4 naïve mice (Table 3). The *pdeB*$^+$ cells' partially restored virulence likely resulted from the overexpression of *pdeB*, or a small population of the complemented *pdeB*$^+$ cells may have lost an endogenous plasmid(s). These results indicated that *pdeB* mutant cells failed to complete the mouse-tick-mouse infection cycle.

***pdeB* mutant cells are deficient in survival in artificially infected ticks.** Tick immersion studies were performed to confirm the extent to which wild-type and mutant *B. burgdorferi* strains are able to infect, survive, and transmit the infection from arthropod tick vectors to a mammalian host (87, 89, 91). Tick immersion studies allow direct artificial tick infection and serve two purposes, i.e., (i) to optimally infect naïve ticks with the wild-type and mutant spirochetes and determine their colonization and the ability to survive within the tick vector and (ii) to examine for the potential of spirochetes to migrate from the arthropod host vector to the mammalian host. Three-month-old tick larvae were artificially inoculated with exponentially growing (5×10^7 cells/ml) cultures of wild-type, *pdeB* mutant, or complemented *pdeB*$^+$ *B. burgdorferi* cells. As ticks ingest *B. burgdorferi* cultures, their intestines are inoculated with spirochetes. After tick immersion, approximately 150 spirochete-laden ticks of each strain were allowed to feed on a naïve mouse ($n = 2$ or 4) (Table 4). Fed ticks were analyzed for the presence of spirochetes by IFA (see Fig. S2 in the supplemental material), and crushed ticks were plated and viable spirochetes were counted. While the spirochete burdens of the ticks inoculated with wild-type or complemented *pdeB*$^+$ cells were approximately the same, the mutant strain spirochete burden was 5-fold lower when ticks were analyzed 7 days after blood acquisition (Table 4). The percentage of fed ticks infected with the wild-type, mutant, or complemented strain was the same (~80%; Table 4). These data and the mouse-tick-mouse results demonstrate that PdeB is likely required for *B. burgdorferi* to colonize and/or survive in the tick vector. Mice on which ticks fed were sacrificed to determine the extent to which spirochetes could be isolated from tissue specimens. Consistent with mouse-tick-mouse infection cycle studies (Table 3), spirochetes were isolated only from tissue specimens collected from mice on which ticks infected with the wild-type or the complemented *pdeB*$^+$ strain fed. No spirochetes were isolated from any of the tissue specimens from mice on which ticks infected with the *pdeB* mutant cells fed (Table 4). These results confirm that the *pdeB* mutant has a reduced ability to colonize ticks and is unable to transmit an infection from ticks to naïve mice.

DISCUSSION

HD-GYP domains belong to the HD superfamily of metal-dependent hydrolases (2, 29–31) and are often encountered fused to other signal transduction domains such as REC, GGDEF, and PAS domains (27, 31). Based on these observations, Galperin et al (31) initially proposed that HD-GYP domain-containing proteins may function as PDEs directed toward either the dephosphorylation of phosphoproteins or the hydrolysis of cyclic nucleotides, especially c-di-GMP. HD-GYP domain-containing proteins subsequently have been shown to indeed possess c-di-GMP-hydrolyzing activity (77, 78). Although more than 590 HD-GYP domains in over 140 genomes have been reported (www.ncbi.nlm.nih.gov/complete_genomes/signalcensus.html), only a handful have been characterized (1, 35, 77, 78). The genome of *B. burgdorferi* encodes a single diguanylate cyclase and two PDEs, one of the EAL type and one of the HD-GYP type (25, 31). Purified recombinant forms of the diguanylate cyclase Rrp1 and the EAL domain-containing PdeA have been shown to synthesize and hydrolyze

TABLE 4. Tick immersion studies indicate the *pdeB* mutant is defective in the ability to colonize ticks and in the ability to transmit the infection from ticks to naïve mice

Strain	% of fed ticks positive for *B. burgdorferi*	Mean no. of spirochetes/tick ± SD	No. of mice infected/total
Wild type	88	3,366 ± 1,750	2/2
pdeB mutant	80	618 ± 837	0/4
Complemented *pdeB*$^+$	75	3,460 ± 1,975	2/2

c-di-GMP *in vitro*, respectively (81, 91). In PDE assays, extracts from *pdeA* mutant cells exhibited a reduced ability to hydrolyze ^{33}P-labeled c-di-GMP, relative to that of wild-type cells. However, *pdeA* mutant cell extracts retained considerable c-di-GMP-hydrolyzing activity, leading us to propose that *B. burgdorferi* expresses more than one functional PDE (91). Several lines of evidence led us to conclude that the HD-GYP domain-containing protein PdeB functions as a c-di-GMP-specific PDE (Fig. 4A to C). First, we constructed a *pdeB* mutant of *B. burgdorferi* and compared the abilities of extracts from wild-type, mutant, and complemented cells to hydrolyze radiolabeled c-di-GMP *in vitro*. The wild-type and complemented cell extracts readily hydrolyzed ^{33}P-labeled c-di-GMP, and this activity was reduced in extracts from *pdeB* mutants (Fig. 4A). Second, purified recombinant full-length protein and a truncated form of PdeB containing the HD-GYP domain exhibit c-di-GMP-specific PDE activity (Fig. 4B and C); as with other HD-GYP PDEs, the activity of PdeB was enhanced by the addition of Mn^{2+} (77, 78, 94). It is notable that when the HD-GYP domain of RpfG of *X. campestris* was mutated to HA-GYP, the c-di-GMP-hydrolyzing activity was abolished (77). *B. burgdorferi* PdeB contains an imperfect HK-GYP domain instead of HD-GYP; it is not known if a mutation in the HD-GYP domain of RpfG to HK-GYP would alter enzyme activity. However, our PDE assays clearly demonstrate that the HK-GYP domain-containing PdeB hydrolyzes c-di-GMP and exhibits a high affinity for c-di-GMP (Fig. 4A to C).

To date, only three HD-GYP-type PDEs have been shown to hydrolyze c-di-GMP in bacteria; however, K_m values for those PDEs have not been reported (77, 78). Here, we determined that the K_m for PdeB is 2.9 nM, a value which is substantially lower than those previously reported for EAL-type PDEs (60 nM to a few micromolar) (36, 91, 94). Bioinformatic analysis suggests that PdeA and PdeB are the only PDEs in *B. burgdorferi* (31). Consistent with this notion, cell extracts prepared from the wild type, the single mutants (*pdeA* and *pdeB*), or their complements hydrolyzed ^{33}P-labeled c-di-GMP within 2 to 20 min of incubation, while extracts prepared from spirochetes lacking both PdeA and PdeB failed to hydrolyze the nucleotide even when the reaction mixtures were incubated for up to 4 h (Fig. 4A and reference 91).

Similar to their EAL-type counterparts (39, 94, 96), HD-GYP-type PDEs have been implicated in motility regulation in *P. aeruginosa* and *X. campestris* (77, 78). Specifically, mutations in the *P. aeruginosa* PDEs *PA4108* and *PA4781* and *X. campestris* pv. *campestris* PDE *rpfG* resulted in reduction of swarming motility (77, 78). Recently, we reported that inactivation of the *B. burgdorferi* EAL-type PdeA rendered spirochetes unable to reverse their direction of swimming (91). Interestingly, the aberrant motility displayed by spirochetes lacking PdeB differed from that of the *pdeA* mutant; PdeB-deficient cells exhibit significantly increased flexing (Table 1). This phenotype was attributed solely to the *pdeB* mutation, since complementation in *trans* restored the wild-type phenotype (Table 1; see Fig. S1 and videos in the supplemental material). Two conditions might be expected to lead to increased flexing, (i) overexpression of CheY3 and (ii) inhibition of CheX activity or decreased expression of CheX (58, 61, 67). Based on Western blotting, however, both CheY3 and CheX were expressed at wild-type levels in lysates prepared from *pdeB* single and *plzA pdeB* double mutants (Fig. 3), ruling out a direct role for c-di-GMP in regulating the expression of these chemotaxis proteins. Alternatively, c-di-GMP may regulate bacterial motility via an interaction with PilZ proteins (7, 14, 66, 91, 96). *B. burgdorferi* possesses a c-di-GMP-binding PilZ domain protein, PlzA (26, 68). Inactivation of *plzA* results in reduced swarming motility, although the swimming pattern of this mutant was indistinguishable from that of its parent (68). Recently, we demonstrated that the alteration of motility displayed by the *pdeA* mutant (91) is modulated by a PlzA-independent mechanism (68). However, spirochetes lacking PlzA in the *pdeB* mutant background constantly flex, a phenotype that is indistinguishable from that of a *cheX* mutant (see the *cheX* single mutant and *plzA pdeB* double mutant cell videos in the supplemental material) (58). These results suggest that c-di-GMP/PlzA may interact with the *B. burgdorferi* chemotaxis signaling pathway via CheX or CheY3, most likely by modulating the activity of CheX. We hypothesize that when it is not bound to c-di-GMP, PlzA may stimulate CheX activity. Thus, in the *pdeB* mutant, c-di-GMP is elevated, more PlzA–c-di-GMP complex is formed, and CheX activity is diminished, resulting in elevated CheY3-P and increasing the rate of flexing. In the latter scenario, the *plzA pdeB* double mutant would exhibit very low CheX activity, greatly increasing CheY3-P and causing the constant-flexing phenotype. It is possible to test these possibilities using *in vitro* biochemical assays.

It is interesting that *B. burgdorferi* apparently has only two functional c-di-GMP PDEs with disparate motility and virulence phenotypes (91; this study). While both PDEs appear to impact motility, it is unclear how they are able to alter motility in such different ways. Because of their distinct motility phenotypes, it is tempting to speculate that PdeA or PdeB may localize at different poles of a cell, thereby causing the periplasmic flagellar motor rotation to be CW or CCW by interacting with a flagellar protein or modulating the activity of a chemotaxis protein(s) in a manner that is not yet understood. A mutation in *B. burgdorferi pdeA* or *E. coli*/*S. enterica* PDE (*yhjH*) resulted in a biased direction of rotation of flagellar motors and/or decreased flagellar motor rotation. One possibility is that PdeA functions analogously to the EAL-type PDE YhjH in *E. coli* and *S. enterica*. Studies in different laboratories indicated that YhjH alters motility via the c-di-GMP effector protein YcgR, which, when complexed with c-di-GMP, acts as a "brake" on the flagellar motor switch complex (7, 22, 66, 91). However, to our knowledge, this is the first report to demonstrate that *pdeB* mutant cells exhibit a flexing motility phenotype without altering the speed of motor rotations.

In addition to their role in regulating bacterial motility, HD-GYP-type PDEs have also been linked to virulence (76, 79, 96). Recently, we demonstrated that spirochetes lacking PdeA were unable to infect mice following needle or tick inoculation, presumably as a result of their failure to reverse swimming direction (91). Loss of PdeB, on the other hand, had no significant effect on virulence ($P = 0.3976$), further supporting our hypothesis that PdeA and PdeB exert their regulatory effects by independent mechanisms. Recently, independent studies by Caimano et al. (10a), He et al. (35a), and Kostick et al. (45) demonstrated that *hk1* and *rrp1* are required for survival within fed tick midguts. Survival of the *rrp1* mutant could be partially restored in feeding ticks by constitutive expression

of genes involved in glycerol uptake and utilization (*glp* genes) (X. F. Yang, personal communication) (35a). Interestingly, spirochetes lacking *pdeB* also displayed a survival defect within fed ticks, although the mechanism(s) underlying the phenotype observed with our *pdeB* mutant differs from that of *hk1* and *rrp1* mutants; unlike *hk1*/*rrp1* mutants, which are killed early (within 36 h) during the blood meal, spirochetes lacking PdeB appear to be killed postrepletion. Not surprisingly, loss of *pdeB* had no effect on *glp* gene (*bb0241* and *bb0243*) expression *in vitro* (our unpublished observation). Together, these data may indicate that a precise modulation of c-di-GMP levels is central to the tick phase of the spirochete's enzootic cycle, with increased and decreased levels of c-di-GMP being required for adaptation to the fed and flat tick midgut environments, respectively. Somewhat surprisingly, nymphal ticks infected with the *pdeB* mutant failed to transmit the infection to naïve mice during engorgement, despite containing substantial numbers of viable spirochetes (Table 3). The latter data suggest a potential role for decreased c-di-GMP levels in promoting the migration of spirochetes out of the midgut during feeding. The decreased ability of PdeB-deficient spirochetes to survive within replete ticks may suggest that the degradation of c-di-GMP controls the expression and/or activity of *B. burgdorferi* gene products required to withstand growth within the flat midgut environment. Recently, constructed *bb0323*, *bb0365*, *guaAB*, *dps*, *ospA*/*B*, and *bptA* mutant strains exhibited defects in the ability to survive in ticks (41, 53, 64, 68, 73, 98, 99). Furthermore, the *bba52*, *bba64*, or *bba07* mutant was reported to be unable to transmit spirochetes from ticks to naïve mice, although each of the mutants was able to infect mice by needle inoculation (32, 48, 97). Whether c-di-GMP affected the expression of one or more of these or other *B. burgdorferi* genes remains to be investigated. Clearly, additional studies are required to understand the unusual and complicated signaling produced by c-di-GMP-metabolizing proteins.

ACKNOWLEDGMENTS

We thank Melissa Caimano, Justin Radolf, and X. Frank Yang for sharing their unpublished results and Nyles Charon, Justin Radolf, and Melissa Caimano for comments on the manuscript. We thank C. Li, R. Rego, P. Rosa, B. Stevenson, V. T. Lee, A. Camilli, D. Blair, A. Barbour, J. Benach, and J. Carroll for providing reagents. We also thank D. Akins for *B. burgdorferi* plasmid primer sequence information.

This research is sponsored by an East Carolina University Research and Development "start-up" fund to M.A.M.

REFERENCES

1. **Andrade, M. O., et al.** 2006. The HD-GYP domain of RpfG mediates a direct linkage between the Rpf quorum-sensing pathway and a subset of diguanylate cyclase proteins in the phytopathogen *Xanthomonas axonopodis* pv *citri*. Mol. Microbiol. **62:**537–551.
2. **Aravind, L., and E. V. Koonin.** 1998. The HD domain defines a new superfamily of metal-dependent phosphohydrolases. Trends Biochem. Sci. **23:**469–472.
3. **Armitage, J. P., and R. M. Berry.** 2010. Time for bacteria to slow down. Cell **141:**24–26.
4. **Babb, K., K. von Lackum, R. L. Wattier, S. P. Riley, and B. Stevenson.** 2005. Synthesis of autoinducer 2 by the lyme disease spirochete, *Borrelia burgdorferi*. J. Bacteriol. **187:**3079–3087.
5. **Bakker, R. G., C. Li, M. R. Miller, C. Cunningham, and N. W. Charon.** 2007. Identification of specific chemoattractants and genetic complementation of a *Borrelia burgdorferi* chemotaxis mutant: flow cytometry-based capillary tube chemotaxis assay. Appl. Environ. Microbiol. **73:**1180–1188.
6. **Battisti, J. M., et al.** 2008. Outer surface protein A protects Lyme disease spirochetes from acquired host immunity in the tick vector. Infect. Immun. **76:**5228–5237.
7. **Boehm, A., et al.** 2010. Second messenger-mediated adjustment of bacterial swimming velocity. Cell **141:**107–116.
8. **Boesch, K. C., R. E. Silversmith, and R. B. Bourret.** 2000. Isolation and characterization of nonchemotactic CheZ mutants of *Escherichia coli*. J. Bacteriol. **182:**3544–3552.
9. **Botkin, D. J., et al.** 2006. Identification of potential virulence determinants by Himar1 transposition of infectious *Borrelia burgdorferi* B31. Infect. Immun. **74:**6690–6699.
10. **Butler, S. M., and A. Camilli.** 2004. Both chemotaxis and net motility greatly influence the infectivity of *Vibrio cholerae*. Proc. Natl. Acad. Sci. U. S. A. **101:**5018–5023.

10a. **Caimano, M. J., et al.** 2011. The hybrid histidine kinase Hk1 is part of a two-component system that is essential for survival of *Borrelia burgdorferi* in feeding *Ixodes scapularis* ticks. Infect. Immun. **79:**3117–3130.

11. **Casjens, S., et al.** 2000. A bacterial genome in flux: the twelve linear and nine circular extrachromosomal DNAs in an infectious isolate of the Lyme disease spirochete *Borrelia burgdorferi*. Mol. Microbiol. **35:**490–516.
12. **Charon, N. W., and S. F. Goldstein.** 2002. Genetics of motility and chemotaxis of a fascinating group of bacteria: the spirochetes. Annu. Rev. Genet. **36:**47–73.
13. **Charon, N. W., et al.** 2009. The flat ribbon configuration of the periplasmic flagella of *Borrelia burgdorferi* and its relationship to motility and morphology. J. Bacteriol. **191:**600–607.
14. **Christen, M., et al.** 2007. DgrA is a member of a new family of cyclic diguanosine monophosphate receptors and controls flagellar motor function in *Caulobacter crescentus*. Proc. Natl. Acad. Sci. U. S. A. **104:**4112–4117.
15. **Christen, M., B. Christen, M. Folcher, A. Schauerte, and U. Jenal.** 2005. Identification and characterization of a cyclic di-GMP-specific phosphodiesterase and its allosteric control by GTP. J. Biol. Chem. **280:**30829–30837.
16. **Coleman, J. L., and J. L. Benach.** 1992. Characterization of antigenic determinants of *Borrelia burgdorferi* shared by other bacteria. J. Infect. Dis. **165:**658–666.
17. **Cotter, P. A., and S. Stibitz.** 2007. c-di-GMP-mediated regulation of virulence and biofilm formation. Curr. Opin. Microbiol. **10:**17–23.
18. **Dombrowski, C., et al.** 2009. The elastic basis for the shape of *Borrelia burgdorferi*. Biophys. J. **96:**4409–4417.
19. **Dunham-Ems, S. M., et al.** 2009. Live imaging reveals a biphasic mode of dissemination of *Borrelia burgdorferi* within ticks. J. Clin. Invest. **119:**3652–3665.
20. **Elias, A. F., et al.** 2003. New antibiotic resistance cassettes suitable for genetic studies in *Borrelia burgdorferi*. J. Mol. Microbiol. Biotechnol. **6:**29–40.
21. **Elias, A. F., et al.** 2002. Clonal polymorphism of *Borrelia burgdorferi* strain B31 MI: implications for mutagenesis in an infectious strain background. Infect. Immun. **70:**2139–2150.
22. **Fang, X., and M. Gomelsky.** 2010. A posttranslational, c-di-GMP-dependent mechanism regulating flagellar motility. Mol. Microbiol. **76:**1295–1305.
23. **Fosnaugh, K., and E. P. Greenberg.** 1988. Motility and chemotaxis of *Spirochaeta aurantia*: computer-assisted motion analysis. J. Bacteriol. **170:**1768–1774.
24. **Frank, K. L., S. F. Bundle, M. E. Kresge, C. H. Eggers, and D. S. Samuels.** 2003. *aadA* confers streptomycin resistance in *Borrelia burgdorferi*. J. Bacteriol. **185:**6723–6727.
25. **Fraser, C. M., et al.** 1997. Genomic sequence of a Lyme disease spirochaete, *Borrelia burgdorferi*. Nature **390:**580–586.
26. **Freedman, J. C., et al.** 2010. Identification and molecular characterization of a cyclic-di-GMP effector protein, PlzA (BB0733): additional evidence for the existence of a functional cyclic-di-GMP regulatory network in the Lyme disease spirochete, *Borrelia burgdorferi*. FEMS Immunol. Med. Microbiol. **58:**285–294.
27. **Galperin, M. Y.** 2004. Bacterial signal transduction network in a genomic perspective. Environ. Microbiol. **6:**552–567.
28. **Galperin, M. Y.** 2005. A census of membrane-bound and intracellular signal transduction proteins in bacteria: bacterial IQ, extroverts and introverts. BMC Microbiol. **5:**35.
29. **Galperin, M. Y.** 2010. Diversity of structure and function of response regulator output domains. Curr. Opin. Microbiol. **13:**150–159.
30. **Galperin, M. Y., D. A. Natale, L. Aravind, and E. V. Koonin.** 1999. A specialized version of the HD hydrolase domain implicated in signal transduction. J. Mol. Microbiol. Biotechnol. **1:**303–305.
31. **Galperin, M. Y., A. N. Nikolskaya, and E. V. Koonin.** 2001. Novel domains of the prokaryotic two-component signal transduction systems. FEMS Microbiol. Lett. **203:**11–21.
32. **Gilmore, R. D., Jr, et al.** 2010. The *bba64* gene of *Borrelia burgdorferi*, the Lyme disease agent, is critical for mammalian infection via tick bite transmission. Proc. Natl. Acad. Sci. U. S. A. **107:**7515–7520.
33. **Goldstein, S. F., N. W. Charon, and J. A. Kreiling.** 1994. *Borrelia burgdorferi* swims with a planar waveform similar to that of eukaryotic flagella. Proc. Natl. Acad. Sci. U. S. A. **91:**3433–3437.
34. **Goldstein, S. F., et al.** 2010. The chic motility and chemotaxis of *Borrelia*

burgdorferi, p. 161–181. *In* D. S. Samuels and J. D. Radolf (ed.), *Borrelia*: molecular biology, host interactions and pathogenesis. Caister Academic Press. Norfolk, United Kingdom.

35. **Hammer, B. K., and B. L. Bassler.** 2009. Distinct sensory pathways in *Vibrio cholerae* El Tor and classical biotypes modulate cyclic dimeric GMP levels to control biofilm formation. J. Bacteriol. **191:**169–177.

35a. **He, M., et al.** Cyclic-di-GMP is essential for the survival of the Lyme disease spirochete in ticks. PLoS Pathog., in press.

36. **Hengge, R.** 2009. Principles of c-di-GMP signalling in bacteria. Nat. Rev. Microbiol. **7:**263–273.

37. **Hickman, J. W., and C. S. Harwood.** 2008. Identification of FleQ from *Pseudomonas aeruginosa* as a c-di-GMP-responsive transcription factor. Mol. Microbiol. **69:**376–389.

38. **Hübner, A., A. T. Revel, D. M. Nolen, K. E. Hagman, and M. V. Norgard.** 2003. Expression of a *luxS* gene is not required for *Borrelia burgdorferi* infection of mice via needle inoculation. Infect. Immun. **71:**2892–2896.

39. **Jenal, U., and J. Malone.** 2006. Mechanisms of cyclic-di-GMP signaling in bacteria. Annu. Rev. Genet. **40:**385–407.

40. **Jewett, M. W., et al.** 2007. The critical role of the linear plasmid lp36 in the infectious cycle of *Borrelia burgdorferi*. Mol. Microbiol. **64:**1358–1374.

41. **Jewett, M. W., et al.** 2009. GuaA and GuaB are essential for *Borrelia burgdorferi* survival in the tick-mouse infection cycle. J. Bacteriol. **191:**6231–6241.

42. **Josenhans, C., and S. Suerbaum.** 2002. The role of motility as a virulence factor in bacteria. Int. J. Med. Microbiol. **291:**605–614.

43. **Kawabata, H., S. J. Norris, and H. Watanabe.** 2004. BBE02 disruption mutants of *Borrelia burgdorferi* B31 have a highly transformable, infectious phenotype. Infect. Immun. **72:**7147–7154.

44. **Kimsey, R. B., and A. Spielman.** 1990. Motility of Lyme disease spirochetes in fluids as viscous as the extracellular matrix. J. Infect. Dis. **162:**1205–1208.

45. **Kostick, J. L., et al.** 4 May 2011, posting date. The diguanylate cyclase, Rrp1, regulates critical steps in the enzootic cycle of the Lyme disease spirochetes. Mol. Microbiol. [Epub ahead of print.] doi:10.1111/j.1365-2958.2011.07687.x.

46. **Kudryashev, M., et al.** 2009. Comparative cryo-electron tomography of pathogenic Lyme disease spirochetes. Mol. Microbiol. **71:**1415–1434.

47. **Kulasakara, H., et al.** 2006. Analysis of *Pseudomonas aeruginosa* diguanylate cyclases and phosphodiesterases reveals a role for bis-(3′-5′)-cyclic-GMP in virulence. Proc. Natl. Acad. Sci. U. S. A. **103:**2839–2844.

48. **Kumar, M., X. Yang, A. S. Coleman, and U. Pal.** 2010. BBA52 facilitates *Borrelia burgdorferi* transmission from feeding ticks to murine hosts. J. Infect. Dis. **201:**1084–1095.

49. **Lai, T. H., Y. Kumagai, M. Hyodo, Y. Hayakawa, and Y. Rikihisa.** 2009. The *Anaplasma phagocytophilum* PleC histidine kinase and PleD diguanylate cyclase two-component system and role of cyclic di-GMP in host cell infection. J. Bacteriol. **191:**693–700.

50. **Li, C., et al.** 2002. Asymmetrical flagellar rotation in *Borrelia burgdorferi* nonchemotactic mutants. Proc. Natl. Acad. Sci. U. S. A. **99:**6169–6174.

51. **Li, C., M. A. Motaleb, M. Sal, S. F. Goldstein, and N. W. Charon.** 2000. Spirochete periplasmic flagella and motility. J. Mol. Microbiol. Biotechnol. **2:**345–354.

52. **Li, C., H. Xu, K. Zhang, and F. T. Liang.** 2010. Inactivation of a putative flagellar motor switch protein FliG1 prevents *Borrelia burgdorferi* from swimming in highly viscous media and blocks its infectivity. Mol. Microbiol. **75:**1563–1576.

53. **Li, X., et al.** 2007. The Lyme disease agent *Borrelia burgdorferi* requires BB0690, a Dps homologue, to persist within ticks. Mol. Microbiol. **63:**694–710.

54. **Livak, K. J., and T. D. Schmittgen.** 2001. Analysis of relative gene expression data using real-time quantitative PCR and the 2(-Delta Delta C(T)) method. Methods **25:**402–408.

55. **Moisi, M., et al.** 2009. A novel regulatory protein involved in motility of *Vibrio cholerae*. J. Bacteriol. **191:**7027–7038.

56. **Motaleb, M. A., et al.** 2000. *Borrelia burgdorferi* periplasmic flagella have both skeletal and motility functions. Proc. Natl. Acad. Sci. U. S. A. **97:**10899–10904.

57. **Motaleb, M. A., M. R. Miller, R. G. Bakker, C. Li, and N. W. Charon.** 2007. Isolation and characterization of chemotaxis mutants of the Lyme disease spirochete *Borrelia burgdorferi* using allelic exchange mutagenesis, flow cytometry, and cell tracking. Methods Enzymol. **422:**421–437.

58. **Motaleb, M. A., et al.** 2005. CheX is a phosphorylated CheY phosphatase essential for *Borrelia burgdorferi* chemotaxis. J. Bacteriol. **187:**7963–7969.

59. **Motaleb, M. A., J. E. Pitzer, S. Z. Sultan, and J. Liu.** 25 March 2011, posting date. A novel gene inactivation system reveals an altered periplasmic flagellar orientation in a *Borrelia burgdorferi fliL* mutant. J. Bacteriol. [Epub ahead of print.]

60. **Motaleb, M. A., M. S. Sal, and N. W. Charon.** 2004. The decrease in FlaA observed in a flaB mutant of *Borrelia burgdorferi* occurs posttranscriptionally. J. Bacteriol. **186:**3703–3711.

61. **Motaleb, M. A., S. Z. Sultan, M. R. Miller, C. Li, and N. W. Charon.** 29 April 2011, posting date. CheY3 of *Borrelia burgdorferi* is the key response regulator essential for chemotaxis and forms a long-lived phosphorylated intermediate. J. Bacteriol. [Epub ahead of print.]

62. **Ottemann, K. M., and A. C. Lowenthal.** 2002. *Helicobacter pylori* uses motility for initial colonization and to attain robust infection. Infect. Immun. **70:**1984–1990.

63. **Ouyang, Z., et al.** 2009. BosR (BB0647) governs virulence expression in *Borrelia burgdorferi*. Mol. Microbiol. **74:**1331–1343.

64. **Pal, U., et al.** 2008. A differential role for BB0365 in the persistence of *Borrelia burgdorferi* in mice and ticks. J. Infect. Dis. **197:**148–155.

65. **Parveen, N., and K. A. Cornell.** 2011. Methylthioadenosine/S-adenosylhomocysteine nucleosidase, a critical enzyme for bacterial metabolism. Mol. Microbiol. **79:**7–20.

66. **Paul, K., V. Nieto, W. C. Carlquist, D. F. Blair, and R. M. Harshey.** 2010. The c-di-GMP binding protein YcgR controls flagellar motor direction and speed to affect chemotaxis by a "backstop brake" mechanism. Mol. Cell **38:**128–139.

67. **Pazy, Y., et al.** 2010. Identical phosphatase mechanisms achieved through distinct modes of binding phosphoprotein substrate. Proc. Natl. Acad. Sci. U. S. A. **107:**1924–1929.

68. **Pitzer, J. E., et al.** 2011. Analysis of the *Borrelia burgdorferi* cyclic-di-GMP binding protein PlzA reveals a role in motility and virulence. Infect. Immun. **79:**1815–1825.

69. **Policastro, P. F., and T. G. Schwan.** 2003. Experimental infection of *Ixodes scapularis* larvae (Acari: Ixodidae) by immersion in low passage cultures of *Borrelia burgdorferi*. J. Med. Entomol. **40:**364–370.

70. **Purser, J. E., and S. J. Norris.** 2000. Correlation between plasmid content and infectivity in *Borrelia burgdorferi*. Proc. Natl. Acad. Sci. U. S. A. **97:**13865–13870.

71. **Reed, L. J., and H. Muench.** 1938. A simple method of estimating fifty percent endpoints. Am. J. Hyg. **27:**493–497.

72. **Rego, R. O., A. Bestor, and P. A. Rosa.** 2011. Defining the plasmid-encoded restriction-modification systems of the Lyme disease spirochete *Borrelia burgdorferi*. J. Bacteriol. **193:**1161–1171.

73. **Revel, A. T., et al.** 2005. *bptA* (*bbe16*) is essential for the persistence of the Lyme disease spirochete, Borrelia burgdorferi, in its natural tick vector. Proc. Natl. Acad. Sci. U. S. A. **102:**6972–6977.

74. **Riley, S. P., T. Bykowski, K. Babb, K. von Lackum, and B. Stevenson.** 2007. Genetic and physiological characterization of the *Borrelia burgdorferi* ORF *BB0374-pfs-metK-luxS* operon. Microbiology **153:**2304–2311.

75. **Rogers, E. A., et al.** 2009. Rrp1, a cyclic-di-GMP-producing response regulator, is an important regulator of *Borrelia burgdorferi* core cellular functions. Mol. Microbiol. **71:**1551–1573.

76. **Römling, U., and R. Simm.** 2009. Prevailing concepts of c-di-GMP signaling. Contrib. Microbiol. **16:**161–181.

77. **Ryan, R. P., et al.** 2006. Cell-cell signaling in *Xanthomonas campestris* involves an HD-GYP domain protein that functions in cyclic di-GMP turnover. Proc. Natl. Acad. Sci. U. S. A. **103:**6712–6717.

78. **Ryan, R. P., et al.** 2009. HD-GYP domain proteins regulate biofilm formation and virulence in *Pseudomonas aeruginosa*. Environ. Microbiol. **11:**1126–1136.

79. **Ryan, R. P., et al.** 2010. Cell-cell signal-dependent dynamic interactions between HD-GYP and GGDEF domain proteins mediate virulence in *Xanthomonas campestris*. Proc. Natl. Acad. Sci. U. S. A. **107:**5989–5994.

80. **Ryjenkov, D. A., R. Simm, U. Römling, and M. Gomelsky.** 2006. The PilZ domain is a receptor for the second messenger c-di-GMP: the PilZ domain protein YcgR controls motility in enterobacteria. J. Biol. Chem. **281:**30310–30314.

81. **Ryjenkov, D. A., M. Tarutina, O. V. Moskvin, and M. Gomelsky.** 2005. Cyclic diguanylate is a ubiquitous signaling molecule in bacteria: insights into biochemistry of the GGDEF protein domain. J. Bacteriol. **187:**1792–1798.

82. **Sal, M. S., et al.** 2008. *Borrelia burgdorferi* uniquely regulates its motility genes and has an intricate flagellar hook-basal body structure. J. Bacteriol. **190:**1912–1921.

83. **Schirmer, T., and U. Jenal.** 2009. Structural and mechanistic determinants of c-di-GMP signalling. Nat. Rev. Microbiol. **7:**724–735.

84. **Simm, R., U. Remminghorst, I. Ahmad, K. Zakikhany, and U. Römling.** 2009. A role for the EAL-like protein STM1344 in regulation of CsgD expression and motility in *Salmonella enterica* serovar Typhimurium. J. Bacteriol. **191:**3928–3937.

85. **Simpson, W. J., W. Burgdorfer, M. E. Schrumpf, R. H. Karstens, and T. G. Schwan.** 1991. Antibody to a 39-kilodalton *Borrelia burgdorferi* antigen (P39) as a marker for infection in experimentally and naturally inoculated animals. J. Clin. Microbiol. **29:**236–243.

86. **Steere, A. C., J. Coburn, and L. Glickstein.** 2004. The emergence of Lyme disease. J. Clin. Invest. **113:**1093–1101.

87. **Stewart, P. E., A. Bestor, J. N. Cullen, and P. A. Rosa.** 2008. A tightly regulated surface protein of *Borrelia burgdorferi* is not essential to the mouse-tick infectious cycle. Infect. Immun. **76:**1970–1978.

88. **Stewart, P. E., R. Thalken, J. L. Bono, and P. Rosa.** 2001. Isolation of a circular plasmid region sufficient for autonomous replication and transformation of infectious Borrelia burgdorferi. Mol. Microbiol. **39:**714–721.

89. **Strother, K. O., and A. de Silva.** 2005. Role of *Borrelia burgdorferi* linear plasmid 25 in infection of *Ixodes scapularis* ticks. J. Bacteriol. **187:**5776–5781.
90. **Sudarsan, N., et al.** 2008. Riboswitches in eubacteria sense the second messenger cyclic di-GMP. Science **321:**411–413.
91. **Sultan, S. Z., J. E. Pitzer, M. R. Miller, and M. A. Motaleb.** 2010. Analysis of a *Borrelia burgdorferi* phosphodiesterase demonstrates a role for cyclic-di-GMP in motility and virulence. Mol. Microbiol. **77:**128–142.
92. **Tamayo, R., J. T. Pratt, and A. Camilli.** 2007. Roles of cyclic diguanylate in the regulation of bacterial pathogenesis. Annu. Rev. Microbiol. **61:**131–148.
93. **Tamayo, R., S. Schild, J. T. Pratt, and A. Camilli.** 2008. Role of cyclic di-GMP during El Tor biotype *Vibrio cholerae i*nfection: characterization of the in vivo-induced cyclic di-GMP phosphodiesterase CdpA. Infect. Immun. **76:**1617–1627.
94. **Tamayo, R., A. D. Tischler, and A. Camilli.** 2005. The EAL domain protein VieA is a cyclic diguanylate phosphodiesterase. J. Biol. Chem. **280:**33324–33330.
95. **Tilly, K., et al.** 2006. *Borrelia burgdorferi* OspC protein required exclusively in a crucial early stage of mammalian infection. Infect. Immun. **74:**3554–3564.
96. **Wolfe, A. J., and K. L. Visick.** 2008. Get the message out: cyclic-di-GMP regulates multiple levels of flagellum-based motility. J. Bacteriol. **190:**463–475.
97. **Xu, H., M. He, J. J. He, and X. F. Yang.** 2010. Role of the surface lipoprotein BBA07 in the enzootic cycle of *Borrelia burgdorferi*. Infect. Immun. **78:**2910–2918.
98. **Yang, X. F., U. Pal, S. M. Alani, E. Fikrig, and M. V. Norgard.** 2004. Essential role for OspA/B in the life cycle of the Lyme disease spirochete. J. Exp. Med. **199:**641–648.
99. **Zhang, X., X. Yang, M. Kumar, and U. Pal.** 2009. BB0323 function is essential for *Borrelia burgdorferi* virulence and persistence through tick-rodent transmission cycle. J. Infect. Dis. **200:**1318–1330.
100. **Zhou, X., M. R. Miller, M. Motaleb, N. W. Charon, and P. He.** 2008. Spent culture medium from virulent *Borrelia burgdorferi* increases permeability of individually perfused microvessels of rat mesentery. PLoS One **3:**e4101.

Editor: A. Camilli